Phase transitions and soft modes in ferroelectric superlattices

1990 J. Phys.: Condens. Matter 2 5409

(http://iopscience.iop.org/0953-8984/2/24/013)

J. Phys.: Condens. Matter 2 (1990) 5409–5431. Printed in the UK

Phase transitions and soft modes in ferroelectric superlattices

D Schwenk, F Fishman and F Schwabl
Institut für Theoretische Physik, Physik-Department der Technischen Universität München, D-8046 Garching, Federal Republic of Germany

Received 22 September 1989

Abstract. A theory of periodic ferroelectric multilayers is presented. The multilayer system consists of two alternating ferroelectrics with different transition temperatures. The system is described by a Ginzburg–Landau functional with space-dependent coefficients. In particular, we consider the case of a ferroelectric phase transition of first order. Expressions for static properties such as transition temperature, supercooling temperature and polarisation profile are derived. Immediately below the transition temperature there are unpolarised domains within the stronger ferroelectric layers. Their existence is due to the possible phase coexistence of the ordered and disordered phases in the corresponding bulk material. In order to describe the soft-mode dynamics we use phenomenological equations of motion and study the spectrum of transverse optical modes. The lowest bands are almost dispersion-free and the corresponding modes are confined to those layers which have the lower bulk soft-mode frequency. Because the bulk soft modes of the two layers soften at different temperatures the localisation of the modes in one or the other layer depends upon the temperature. This temperature dependence of the mode form can be seen in the lineshape of the polarisation correlation function if the soft-mode damping of the two layers is different. Furthermore, interface modes are shown to exist. Their energy lies below the continuum, confined by the two bulk soft-mode frequencies. These modes result from the special form of the inhomogeneous polarisation profile in a superlattice in contrast to the Fuchs–Kliever interface modes, which have their origin in the long-range dipolar interaction. The number of these bound states depends on the temperature.

1. Introduction

Nowadays the fabrication of artificial heterostructures down to atomic dimensions is possible. A great number of different types of layer structures, which differ by the nature of their constituents, has been realised. Much interest has been focused on combinations of semiconducting, metallic, magnetic and superconducting materials. In this article we will study ferroelectric heterostructures. Experiments on these structures are still in their infancy. We are aware only of superlattices made of the ferroelectric IV–VI compounds GeTe, SnTe and PbTe [1–3]. However, mainly the electronic properties of these semiconducting materials were studied.

Ferroelectric multilayers are of interest because possible device applications are conceivable in the classical fields of ferroelectric applications such as pyroelectric detection, memory systems or electro-optic modulators. But there is also fundamental interest in the study of these artificial structures, because their properties can differ drastically from the bulk ones.

0953-8984/90/245409 + 23 $03.50

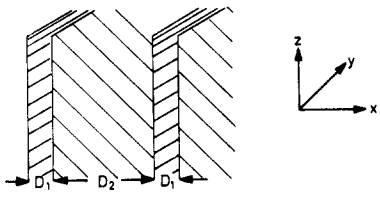

Figure 1. Geometry of the periodic layer structure. Thicknesses of layers 1 and 2 are D_1 and D_2.

We present a continuum theory of the statics and dynamics of ferroelectric superlattices starting from an inhomogeneous Ginzburg–Landau (GL) energy functional. The advantage of the GL theory is that a variety of physical properties are described without referring in detail to all the degrees of freedom of the system. The mathematical simplicity results from Landau's order-parameter concept. The order parameter of the ferroelectric is the polarisation density. The GL theory is not specific to particular materials and can be applied equally well to other multilayer structures undergoing a phase transition, e.g. ferromagnets.

We will study heterostructures undergoing a phase transition of first order, while transitions of second order have been treated in [4]. We address the following questions: (i) what are the phase transition and the supercooling temperatures of the structure and (ii) what is the polarisation profile? We also incorporate interface effects, which may arise due to structural and electronic mismatch at the interfaces. We will characterise these effects by a phenomenological interface-energy term in the GL functional.

A major part of this work is devoted to the soft optical lattice modes in these structures, which are closely connected via the Lyddane–Sachs–Teller relation to the statics of the ferroelectric phase transition. The dynamic part of our theory is based on a phenomenological equation of motion, which was introduced by Ginzburg [5]. In the study of the dynamic properties the following questions are of special interest: (i) what is the detailed 'miniband' structure of the superlattice soft-mode spectrum and are the corresponding modes localised or extended, and (ii) how does the long-range dipolar interaction influence the spectrum?

We are also interested in the lineshape of the dynamic correlation function, which may be probed in Raman or neutron scattering experiments.

The outline of this paper is as follows. In section 2, we describe the model and the GL energy functional. In section 3, the polarisation profile and the transition temperature will be derived from the GL equation. In section 4, we consider the dynamics of the system, and in section 5, we analyse the dynamic correlation functions. In section 6, the results are summarised.

2. The model

We consider a composite material made of two periodically arranged ferroelectric layers, as shown in figure 1. The interfaces between the layers define the yz planes. The widths of the layers are D_1 and D_2 and hence the period of the heterostructure is $D = D_1 + D_2$. The study of the static and dynamic properties of this composite material will be based on the Ginzburg–Landau (GL) theory and hence we start with a discussion of the appropriate GL functional. We consider only proper ferroelectrics, where the local polarisation $\boldsymbol{P}(\boldsymbol{x})$ can be taken as the order parameter. We also assume that both ferroelectrics undergo a first-order phase transition and have cubic symmetry in the

disordered phase. The interfaces correspond to (100) planes. Examples of such ferroelectrics are $BaTiO_3$ and $PbTiO_3$, whose material parameters will be used later in the numerical calculations (cf appendix 1). However, we would like to emphasise that our theory is material-independent and can be applied to other ferroelectric materials as well. Of course, if the constituents have a different symmetry, the GL functional should be modified accordingly.

In the absence of any external electric field the GL functional may be expressed in terms of the local polarisation $\boldsymbol{P}$ and the strain e_i [6]:

$$G(T, X_i; \boldsymbol{P}, e_i) = \sum_{i=1}^{4} G_i - \int \left(\tfrac{1}{2}\boldsymbol{E}^{\mathrm{m}} \cdot \boldsymbol{P} + \sum_{i=1}^{6} X_i e_i \right) \mathrm{d}^3 x. \tag{2.1}$$

Here we have used the Voigt notation for the components of the strain and stress tensor, i.e. $e_1 = e_{xx}, \ldots, e_4 = e_{xy} + e_{yx}, \ldots, X_1 = X_{xx}, \ldots$ and $X_4 = X_{xy}, \ldots$. In equation (2.1) $\boldsymbol{E}^{\mathrm{m}}$ denotes the depolarisation field. The field obeys the quasi-static Maxwell equations

$$\nabla \times \boldsymbol{E}^{\mathrm{m}} = 0 \tag{2.2a}$$

$$\nabla(\boldsymbol{E}^{\mathrm{m}} + 4\pi \boldsymbol{P}_{\mathrm{tot}}) = 0 \tag{2.2b}$$

where

$$\boldsymbol{P}_{\mathrm{tot}} = \boldsymbol{P} + \frac{\varepsilon_\infty - 1}{4\pi} \boldsymbol{E}^{\mathrm{m}}$$

and $\varepsilon_\infty(\boldsymbol{x})$ is the dielectric permeability.

The potential terms $G_1, \ldots, G_4$ are defined as follows. The first term

$$\begin{aligned} G_1 = \int \Big(& \tfrac{1}{2}a\boldsymbol{P}^2 + \tfrac{1}{4}b_{11} \sum_i P_i^4 + \tfrac{1}{2}b_{12}(P_x^2 P_y^2 + P_y^2 P_z^2 + P_z^2 P_x^2) + \tfrac{1}{8}b_{111} \sum_i P_i^6 \\ & + b_{123} P_x^2 P_y^2 P_z^2 + \tfrac{1}{2}b_{112}[P_x^2(P_y^4 + P_z^4) + P_y^2(P_z^4 + P_x^4) \\ & + P_z^2(P_y^4 + P_x^4)] + \tfrac{1}{2}c_1 \sum_i (\nabla P_i)^2 + \tfrac{1}{2}c_2(\nabla \boldsymbol{P})^2 \\ & - c_3[(\partial_x P_x)(\partial_y P_y) + (\partial_z P_z)(\partial_y P_y) + (\partial_x P_x)(\partial_z P_z)] \Big) \mathrm{d}^3 x \end{aligned} \tag{2.3a}$$

contains the polarisation terms commonly used in the GL expansion. We keep all terms necessary to describe the first-order phase transition in ferroelectrics with cubic symmetry. The second

$$G_2 = \int [\tfrac{1}{2}c_{11}(e_1^2 + e_2^2 + e_3^2) + \tfrac{1}{2}c_{44}(e_4^2 + e_5^2 + e_6^2) + c_{12}(e_1 e_2 + e_1 e_3 + e_3 e_2)] \mathrm{d}^3 x \tag{2.3b}$$

describes the elastic energy of the body. The third

$$\begin{aligned} G_3 = \int \{ & -q_{11}(e_1 P_x^2 + e_2 P_y^2 + e_3 P_z^2) \\ & - q_{12}[e_1(P_y^2 + P_z^2) + e_2(P_x^2 + P_z^2) + e_3(P_y^2 + P_x^2)] \\ & - q_{44}(e_2 P_y P_z + e_3 P_x P_z + e_1 P_y P_x) \} \mathrm{d}^3 x \end{aligned} \tag{2.3c}$$

includes the electrostrictive terms describing coupling between polarisation and strain tensor. Finally,

$$G_4 = \int \{f_{11}(e_1\partial_x P_x + e_2\partial_y P_y + e_3\partial_z P_z) + f_{12}[e_1(\partial_y P_y + \partial_z P_z) + e_2(\partial_x P_x + \partial_z P_z) + e_3(\partial_y P_y + \partial_x P_x)] + f_{44}[e_2(\partial_y P_z + \partial_z P_y) + e_3(\partial_x P_z + \partial_z P_x) + e_1(\partial_y P_x + \partial_x P_y)]\}\, \mathrm{d}^3x \tag{2.3d}$$

are the flexoelectric potential contributions, which we also consider for the sake of completeness. These terms, which are proportional to f_{11}, f_{12} and f_{44} and which couple the derivatives of the polarisation to the strain tensor, are of no importance in the description of static properties of bulk ferroelectrics and are usually omitted. On the other hand, in the heterostructures, where the static polarisation is inhomogeneous, it is known that these terms lead to new effects, such as the appearance of a quadrupole moment under shear stress [7].

Near to the interfaces, the properties of the two materials can differ from those in the bulk. Two important reasons for this can be mismatch of the lattice constants and charge transfer. In order to describe these effects, one can introduce the surface GL functional G_S, which in its simplest form reads

$$G_S = \sum_n G_{S_n} = \sum_n \int \delta(\tfrac{1}{2}D_1 - |x - nD|)[\tfrac{1}{2}JP_x^2 + \tfrac{1}{2}I(P_y^2 + P_z^2)]\, \mathrm{d}^3x. \tag{2.4}$$

We assume that there are no symmetry-breaking fields at the interfaces and hence do not include terms such as $E_i^{\mathrm{surf}}P_i$. If the ferroelectrics contain free carriers, a depletion zone and an additional field E_{depl} will appear near to the interfaces [8]. However, for low carrier concentrations this field is small compared with the characteristic intrinsic field E_{char}, with $E_{\mathrm{char}} \sim aP_0$ since the static susceptibility equals a^{-1}, and can be neglected.

We want to emphasise that all coefficients in the GL functional are defined through the whole sample and are continuous functions of $\boldsymbol{x}$. Far from the interfaces these parameters reach their bulk values $a_\alpha, \ldots$ with $\alpha = 1, 2$. We denote the region where the GL coefficients deviate from their bulk values by Δ. If this transition region Δ is small compared with the correlation length ξ, cf equation (3.8*b*), of the order parameter, one can approximate these coefficients by the discontinuous 'step form' [4]

$$a(\boldsymbol{x}) = \sum_{n=-\infty}^{\infty} \sum_{\alpha=1,2} a_\alpha \Theta\{\tfrac{1}{2}D_\alpha - |x - [n + \tfrac{1}{2}(\alpha - 1)]D|\} \tag{2.5}$$

and similarly for all other GL coefficients. Although this approximation is not essential for our theory, it simplifies the analytical and numerical calculations and will be used below.

As usual in the GL theory we attribute the temperature dependence to $a_\alpha(T)$ in the form

$$a_\alpha(T) = a'_\alpha(T - T_\alpha) \qquad \alpha = 1, 2. \tag{2.6a}$$

For a second-order transition T_α is the transition temperature in the GL approximation, and for a first-order transition it describes the supercooling temperature. The study of

phase transitions in $BaTiO_3$ shows that the experimental data can be fitted well if one assumes that the coefficient b_{11} also depends linearly on the temperature, namely

$$b_{11} = b'_{11}(T - \tilde{T}) \tag{2.6b}$$

with $\tilde{T} = 262$ K [9]. The GL functional (2.1) can be used to describe static as well as dynamic properties of such inhomogeneous ferroelectrics.

3. Transition temperature and polarisation

3.1. Effective Ginzburg–Landau potential

For given temperature T and stress X_i, the equilibrium values $\boldsymbol{P}_0$ and $e_{i,0}$ are obtained by minimising the free energy (2.1) with respect to $\boldsymbol{P}$ and e_i. The minimisation with respect to e_i requires

$$\delta G(T, X_i; \boldsymbol{P}_0, e_{i,0})/\delta e_i = 0. \tag{3.1}$$

Equation (3.1) can be solved for e_i, namely $e_i = e_i(T, X_i; \boldsymbol{P})$. Substituting this solution into (2.1) we obtain the effective static GL functional [10]

$$G^{\mathrm{X}}(T, X_i; \boldsymbol{P}) = \sum_{i=1}^{4} G_i^{\mathrm{X}} + G_{\mathrm{S}} - \int \tfrac{1}{2}\boldsymbol{E}^{\mathrm{m}} \cdot \boldsymbol{P}\, \mathrm{d}^3x. \tag{3.2}$$

Here

$$\begin{aligned} G_1^{\mathrm{X}} = \int \Big(& \tfrac{1}{2}A\boldsymbol{P}^2 + \tfrac{1}{4}B_{11}\sum_i P_i^4 + \tfrac{1}{2}B_{12}(P_x^2P_y^2 + P_y^2P_z^2 + P_z^2P_x^2) \\ & + \tfrac{1}{6}B_{111}\sum_i P_i^6 + B_{123}P_x^2P_y^2P_z^2 + \tfrac{1}{2}B_{112}[P_x^2(P_y^4 + P_z^4) \\ & + P_y^2(P_z^4 + P_x^4) + P_z^2(P_y^4 + P_x^4)] + \tfrac{1}{2}C_1\sum_i (\nabla P_i)^2 + \tfrac{1}{2}C_2(\nabla \boldsymbol{P})^2 \\ & - C_3[(\partial_x P_x)(\partial_y P_y) + (\partial_z P_z)(\partial_y P_y) + (\partial_x P_x)(\partial_z P_z)]\Big)\, \mathrm{d}^3x \end{aligned} \tag{3.3a}$$

describes the potential contribution from the polarisation;

$$\begin{aligned} G_2^{\mathrm{X}} = \int [& -\tfrac{1}{2}s_{11}(X_1^2 + X_2^2 + X_3^2) - \tfrac{1}{2}s_{44}(X_4^2 + X_5^2 + X_6^2) \\ & - s_{12}(X_1X_2 + X_1X_3 + X_3X_2)]\, \mathrm{d}^3x \end{aligned} \tag{3.3b}$$

contains the stress terms;

$$\begin{aligned} G_3^{\mathrm{X}} = \int \{ & -Q_{11}(X_1P_x^2 + X_2P_y^2 + X_3P_z^2) \\ & -Q_{12}[X_1(P_y^2 + P_z^2) + X_2(P_x^2 + P_z^2) + X_3(P_y^2 + P_x^2)] \\ & - Q_{44}(X_4P_yP_z + X_6P_xP_z + X_5P_yP_x)\}\, \mathrm{d}^3x \end{aligned} \tag{3.3c}$$

describes the interaction between stress and polarisation; and

$$\begin{aligned} G_4^{\mathrm{X}} = \int \{ & F_{11}(X_1\partial_x P_x + X_2\partial_y P_y + X_3\partial_z P_z) \\ & + F_{12}[X_1(\partial_y P_y + \partial_z P_z) + X_2(\partial_x P_x + \partial_z P_z) + X_3(\partial_y P_y + \partial_x P_x)] \end{aligned}$$

$$+ F_{44}[X_5(\partial_y P_z + \partial_z P_y) + X_6(\partial_x P_z + \partial_z P_x)$$
$$+ X_4(\partial_y P_x + \partial_x P_y)]\}\, \mathrm{d}^3x \tag{3.3d}$$

couples the stress to the derivatives of the polarisation.

The GL coefficients A, B_{11}, . . ., which appear in this effective functional, are given in terms of the original coefficients a, b_{11}, . . . in appendix 2.

3.2. Ginzburg–Landau equation

It is well known [9] that the spontaneous polarisation in $BaTiO_3$ and $PbTiO_3$ is oriented along either a (001), (011) or (111) axis depending upon the temperature range. We will only consider temperatures above room temperature, where the easy axes of both $BaTiO_3$ and $PbTiO_3$ are along the (001) direction. Hence we can assume that in the multilayer the transition occurs into the (001) phase.

In the following we consider the composite material in the form of a slab with dimensions L_y, $L_z \gg L_x$. Keeping in mind that $\boldsymbol{P}_0$ depends only on x, we can easily see that the solution of the Maxwell equations (2.2) in this geometry is

$$\boldsymbol{E}_0^{\mathrm{m}} = \left(-\frac{4\pi}{\varepsilon_\infty} P_{0,x}, 0, 0\right) \tag{3.4}$$

which obviously satisfies the electromagnetic boundary conditions. Therefore the term $-\boldsymbol{P}_0 \cdot \boldsymbol{E}_0^{\mathrm{m}}$ in the GL functional is minimal (as well as the functional itself) for $P_{0,x} = 0$ and we can take $\boldsymbol{P}_0(x)$ to be oriented along the z axis, namely

$$\boldsymbol{P}_0(x) = P_0(x) \cdot (0, 0, 1). \tag{3.5}$$

Assuming $X_i = 0$ and substituting (3.5) into (3.2), we can now minimise the GL functional to obtain the GL equation in the form

$$\frac{\delta G^{\mathrm{X}}(X_i = 0; P_0)}{\delta P_0}$$
$$= \left(A + \sum_n \delta(\tfrac{1}{2}D_1 - |x - nD|)I + B_{11} P_0^2 + B_{111} P_0^4 - \partial_x C_1 \partial_x\right) P_0 = 0 \tag{3.6}$$

where I is the interface coefficient introduced in (2.4). The polarisation is continuous across the interfaces and integrating (3.6) around $x_n = (\frac{1}{2}D_1 + nD)$ we get also the boundary condition for the derivatives

$$C_1(x_n^-)\partial_x P_0(x_n^-) - C_1(x_n^+)\partial_x P_0(x_n^+) = -IP_0(x_n) \tag{3.7}$$

where x_n^+ (x_n^-) denote the points just right (left) of the interface located at x_n.

The solution of (3.6) is periodic in D and symmetric around $x = 0$ and $x = \frac{1}{2}D$. These conditions define the solution uniquely, which can then be used to calculate the GL functional $G^{\mathrm{X}}(T) = G^{\mathrm{X}}(T; P_0(x))$. Choosing the surface constant $I = 0$ and using the GL parameters representing bulk $BaTiO_3$ and $PbTiO_3$ (cf appendix 1), we solved the GL equation numerically and calculated the corresponding GL functional for $D_1 = D_2 =$

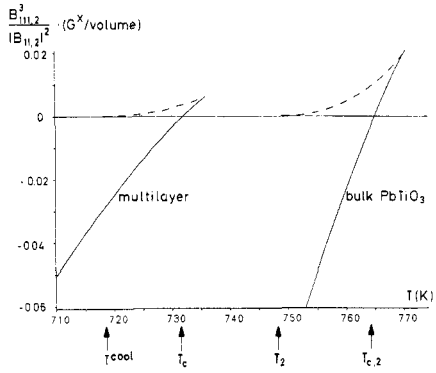

Figure 2. Free energy $G^X(T)$ of the stable (full curves) and unstable (broken curves) phases of the homogeneous system '2' and of the multilayer with parameters given in the appendix and $D_1 = D_2 = 40$ Å.

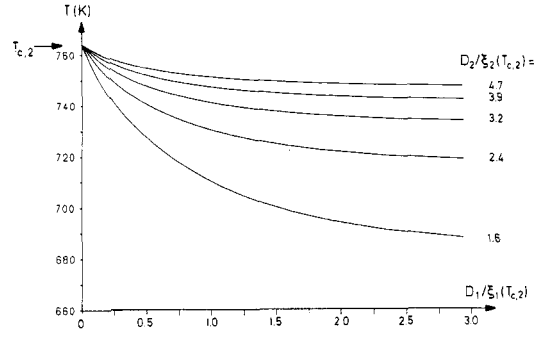

Figure 3. Transition temperature as a function of layer thicknesses.

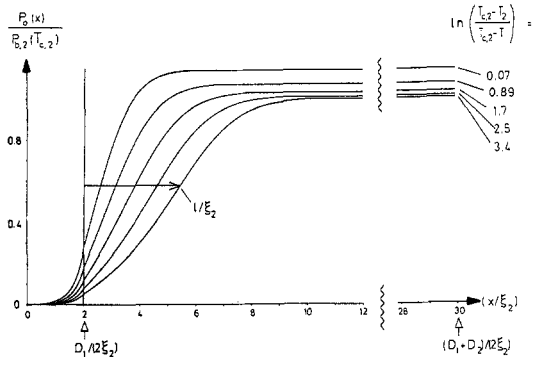

Figure 4. Polarisation profile of a $BaTiO_3/PbTiO_3$ multilayer for different temperatures and $D_1/\xi_2(T_{c,2}) = 4$ and $D_2/\xi_2(T_{c,2}) = 58$.

40 Å. In figure 2 we plot $G^X(T)$ for a heterostructure as well as $G^X_{\text{bulk}}(T)$ for bulk $PbTiO_3$ as functions of temperature. One sees that the behaviour of both functionals is very similar, but the phase transition in the heterostructure (defined by $G^X(T_c) = 0$) occurs at a lower temperature. In figure 3 we show this transition temperature as a function of the layers' thicknesses. For 'thick' high-temperature layers, $D_2 \gg \xi_2(T_{c,2})$, the transition temperature T_c deviates only slightly from $T_{c,2}$, where $\xi_2(T_{c,2})$ is the correlation length, equation (3.8*b*), of the bulk material 2 at its transition temperature $T_{c,2}$ given by

$$T_{c,2} = T_2 + 3B^2_{11,2}/16A'_2B_{111,2}. \tag{3.8a}$$

However, for 'thin' layers, $D_2 \sim \xi_2(T_{c,2})$, the difference can be significant, depending on the thickness of the low-temperature layers.

3.3. Polarisation profile

The general solution of the GL equation (3.6) can be expressed by a combination of elliptic functions [11], which is shown graphically in figure 4. In the case of 'thick' layers,

$D_\alpha \gg \xi_\alpha$, one can express $P_0(x)$ as well as the transition temperature by elementary functions. Here the correlation lengths are defined as

$$\xi_\alpha^{-2} = -[\mathrm{d}V_\alpha^2(P_{b,\alpha})/\mathrm{d}^2 P_{b,\alpha}]/C_{1,\alpha} \tag{3.8b}$$

where $P_{b,\alpha}$ are the bulk polarisations in every constituent material at given temperature and the 'potentials' $V_\alpha(P)$ are

$$V_\alpha(P_0) = -(\tfrac{1}{2}A_\alpha P_0^2 + \tfrac{1}{4}B_{11,\alpha}P_0^4 + \tfrac{1}{6}B_{111,\alpha}P_0^6). \tag{3.9}$$

Let us assume that the parameter I, which describes the surface energy, equation (2.4), satisfies the inequality

$$I > [A_2(T_{c,2})C_{1,2}]^{1/2} - [A_1(T_{c,2})C_{1,1}]^{1/2}. \tag{3.10a}$$

Below we will see that this condition ensures the suppression of polarisation at the interfaces. For 'thick' layers the polarisations in the centre of the layers assume almost their bulk values $P_{b,\alpha}$. In the temperature region $T_1^{heat} < T < T_c$, where

$$T_1^{heat} = T_1 + \frac{B_{11,1}^2}{4A_1' B_{111,1}} \tag{3.10b}$$

is the superheating temperature of the low-temperature ferroelectric [6], we can take $P_{b,1} = 0$ and $P_{b,2} \neq 0$. Then the solution of the GL equation (3.6) can be written as

$$P_0(x) \simeq \Theta(\tfrac{1}{2}D_1 - x)P_1[(\tfrac{1}{2}D_1 - x + \varphi_1)/\xi_1] + \Theta(\tfrac{1}{2}D_2 - |x - \tfrac{1}{2}D|) \times P_2[(x - \tfrac{1}{2}D_1 + \varphi_2)/\xi_2] \qquad 0 < x < \tfrac{1}{2}D \tag{3.11a}$$

where

$$P_1(u) = \{2A_1/[B_{11,1}\sinh^2 u + (4A_1 B_{111,1}/3)^{1/2}\sinh(2u)]\}^{1/2} \qquad u > 0 \tag{3.11b}$$

$$P_2(u) = P_{b,2}\sinh(u/2)/\{\sinh^2(u/2) + [(\tfrac{3}{2}r - 1)/(r - 1)]\}^{1/2} \tag{3.11c}$$

$$r = P_{b,2}^2(T)/P_{b,2}^2(T_{c,2}) \tag{3.11d}$$

and

$$P_{b,2} = \{[-B_{11,2} + (B_{11,2}^2 - 4A_2 B_{111,2})^{1/2}]/2B_{111,2}\}^{1/2}. \tag{3.11e}$$

The constants φ_α are determined by the boundary condition (3.7). For temperatures not far below T_c ($T_2 \ll T < T_c$) we easily obtain from (3.7) the value of the polarisation at the interfaces

$$P_0(D_1/2)^2 = P_{b,2}^2(T_{c,2})A_2'(T_{c,2} - T)/A_2(T_{c,2})(j - 1) \tag{3.12}$$

with

$$j = \frac{A_1(T_{c,2})C_{1,1}}{A_2(T_{c,2})C_{1,2}}\left(1 + \frac{I}{(A_1(T_{c,2})C_{1,1})^{1/2}}\right)^2. \tag{3.13}$$

This result is the generalisation of the known result for a semi-infinite ferroelectric to which it reduces in the limit $C_{1,1} \to 0$ [12]. In the temperature region considered, equation (3.11*c*) can be simplified further and written as

$$P_2(u) = \frac{P_{b,2}(T_{c,2})\sinh(u/2)}{[\sinh^2(u/2) + (T_{c,2} - T_2)/(T_{c,2} - T)]^{1/2}}. \tag{3.14a}$$

It is useful to define a characteristic length

$$l(T) = \xi_2 \ln[(T_{c,2} - T_2)/(T_{c,2} - T)]. \tag{3.14b}$$

We see that the polarisation almost vanishes for $0 < x \ll l + \frac{1}{2}D_1$, but it assumes the bulk

value for $l + \frac{1}{2}D_1 \ll x < \frac{1}{2}D$, as exhibited clearly in figure 4. This coexistence of the two phases with zero and non-zero polarisation was discussed in the literature [11] for semi-infinite media and is a consequence of the first-order phase transition in these materials. In semi-infinite media $l \to \infty$ as the temperature approaches the bulk transition point. In contrast, in the heterostructures this length always remains finite and depends on the thickness of the high-temperature layer. The point is that the above-mentioned 'kink' solution is stable only for temperatures below T_c, the value of which depends on the layer thickness and is lower than $T_{c,2}$.

3.4. Transition temperature

Now we investigate in detail the dependence of the transition temperature on the layer thickness. To this end one substitutes (3.11) into (3.2) and calculates T_c from the condition $G^X(T_c) = 0$. After some algebra one gets

$$(T_{c,2} - T_c)/(T_{c,2} - T_2) = 2\xi_2(T_{c,2})/D_2. \tag{3.15}$$

It follows from equations (3.14*b*) and (3.15) that

$$l(T_c)/D_2 \sim (\xi_2(T_{c,2})/D_2)\ln(D_2/\xi_2(T_{c,2})). \tag{3.16}$$

Although $l(T_c)$ is large compared with the correlation length $\xi_2(T_{c,2})$, it is small in comparison with the layer thickness and thus the layer 2 is largely polarised.

It is also of interest to consider the shift of the supercooling temperature T^{cool} of the heterostructure. Below this temperature the disordered phase $P_0 = 0$ is absolutely unstable. In this sense the supercooling temperature is similar to the transition temperature of a second-order phase transition and hence can be found by a linear stability analysis around $P = 0$ [4]. Using the boundary condition (2.17*b*) and assuming for simplicity $I = 0$, we obtain from the stability analysis the implicit equation for T^{cool}

$$\frac{C_{1,1}}{\xi_{0,1}(T^{cool})}\tanh\left(\frac{D_1}{2\xi_{0,1}(T^{cool})}\right) = \frac{C_{1,2}}{2\xi_{0,2}(T^{cool})}\tan\left(\frac{D_2}{\xi_{0,2}(T^{cool})}\right). \tag{3.17}$$

Here $\xi_{0,\alpha} = (C_{1,\alpha}/|A_\alpha|)^{1/2}$ are the correlation lengths in the disordered phase.

For 'thick' layers it follows from equation (3.17) that

$$(T_2 - T^{cool})/T_2 = (\pi\xi_{0,2}(0)/D_2)^2. \tag{3.18}$$

The shift of the supercooling temperature is smaller than the shift of the transition temperature by a factor of order ξ_2/D_2.

4. Dynamics

4.1. Equation of motion

In this section we consider the dynamics of the order parameter $\boldsymbol{P}$. We refrain from a discussion of the acoustic excitations in superlattices, which have already been studied extensively [13]. The dynamic phenomena in ferroelectrics in general are described by a coupled system of equations of motion for the polarisation $\boldsymbol{P}(\boldsymbol{x}, t)$, the strain components $e_i(\boldsymbol{x}, t)$ and the entropy density $s(\boldsymbol{x}, t)$. However in the low-energy, long-wavelength limit this system of equations can be reduced to a single equation for $\boldsymbol{P}(\boldsymbol{x}, t)$. The reason for this is as follows.

The characteristic timescale of the soft mode ω_0^{-1} is much shorter than the characteristic time for acoustic wave propagation $\omega_a^{-1}(\sim k^{-1})$ and the heat propagation time $\omega_h^{-1}(\sim k^{-2})$. For small wavenumber k these characteristic times obey the inequality

$$\omega_0^{-1} \ll \omega_a^{-1} \ll \omega_h^{-1}. \tag{4.1}$$

Therefore, in this limit one can assume that the soft mode propagates adiabatically at fixed strain, i.e. at the equilibrium value $e_{i,0}$ of strain.

Hence the phenomenological equation that describes the soft-mode propagation reads [10]

$$m(\partial_t^2 + \gamma\partial_t)P_i = -\delta H/\delta P_i. \tag{4.2}$$

Here the adiabatic potential $H = H(s, X_i; \boldsymbol{P}, e_{i,0})$ is related to the previously defined potential $G(T, X_i; \boldsymbol{P}, e_i)$ via the Legendre transform

$$H(s, X_i; \boldsymbol{P}, e_{i,0}) = G(T, X_i; \boldsymbol{P}, e_{i,0}) + \int s(\boldsymbol{x})T(\boldsymbol{x})\,\mathrm{d}^3x \tag{4.3}$$

where

$$s(\boldsymbol{x}) = -\delta G/\delta T(\boldsymbol{x}) \tag{4.4}$$

is the entropy density. In equation (4.2) $m(x)$ is a phenomenological mass parameter with dimension [s^2], while $\gamma(x)$ is a material-dependent damping constant. The depolarisation field $\boldsymbol{E}^m$, which appears in the functional G and in H, correspondingly obeys the quasi-static Maxwell equations (2.2). Equations (4.2) and (2.2) constitute the basic equations of motion for the long-wavelength dynamics of ferroelectric multilayers.

4.2. Harmonic approximation

In order to solve (4.2) in harmonic approximation we linearise around the equilibrium value $\boldsymbol{P}_0$

$$\boldsymbol{P}(\boldsymbol{x}, t) = \boldsymbol{P}_0(\boldsymbol{x}) + \delta\boldsymbol{P}(\boldsymbol{x}, t). \tag{4.5}$$

Then the equation of motion for $\delta\boldsymbol{P}(\boldsymbol{x}, t)$ reads

$$m(\partial_t^2 + \gamma\partial_t)\delta\boldsymbol{P} = -\hat{L}\delta\boldsymbol{P} + \delta\boldsymbol{E}^m \tag{4.6}$$

where the depolarisation field $\delta\boldsymbol{E}^m$ obeys

$$\boldsymbol{\nabla} \times \delta\boldsymbol{E}^m = 0 \tag{4.7a}$$

$$\boldsymbol{\nabla}(\varepsilon_\infty \delta\boldsymbol{E}^m + 4\pi\delta\boldsymbol{P}) = 0 \tag{4.7b}$$

and the linear differential operator $\hat{L}$ is given by

$$\hat{L} = \begin{bmatrix} 1/\chi_\perp^{\mathrm{ad},e_0} - \boldsymbol{\nabla}c_1\boldsymbol{\nabla} - \partial_x c_2 \partial_x & \partial_x(-c_2+c_3)\partial_y & \partial_x(-c_2+c_3)\partial_z \\ \partial_y(-c_2+c_3)\partial_x & 1/\chi_\perp^{\mathrm{ad},e_0} - \boldsymbol{\nabla}c_1\boldsymbol{\nabla} - \partial_y c_2 \partial_y & \partial_y(-c_2+c_3)\partial_z \\ \partial_z(-c_2+c_3)\partial_x & \partial_z(-c_2+c_3)\partial_y & 1/\chi_\parallel^{\mathrm{ad},e_0} - \boldsymbol{\nabla}c_1\boldsymbol{\nabla} - \partial_z c_2 \partial_z \end{bmatrix}. \tag{4.8}$$

Here and in the following we assume for simplicity that the surface terms vanish, i.e.

$I = J = 0$, equation (2.4). In equation (4.8) $\chi_{\perp}^{\mathrm{ad},e_0}(x)$ and $\chi_{\parallel}^{\mathrm{ad},e_0}(x)$ represent the space-dependent transverse and longitudinal local susceptibilities at fixed value of the strain $e_{i,0}$, i.e.

$$1/\chi_{\perp}^{\mathrm{ad},e_0} = A + (B_{12} + q_{44}^2/c_{44})P_0^2 + B_{112}P_0^4 \tag{4.9a}$$

$$1/\chi_{\parallel}^{\mathrm{ad},e_0} = A + 3\tilde{B}_{11}P_0^2 + 5\tilde{B}_{111}P_0^4. \tag{4.9b}$$

Here we introduced

$$\tilde{B}_{11} = B_{11} + (b_{11}^{\mathrm{ad}} - b_{11}) + 4[-4q_{11}q_{12}c_{12} + 2q_{12}^2c_{11} + q_{11}^2(c_{11} + c_{12})] \times [3(c_{11} - c_{12})(c_{11} + 2c_{12})]^{-1} \tag{4.9c}$$

and

$$\tilde{B}_{111} = B_{111} + (b_{111}^{\mathrm{ad}} - b_{111}). \tag{4.9d}$$

The adiabatic GL coefficients b_{11}^{ad} and b_{111}^{ad} appear in (4.9) due to the transformation from the isothermal potential G to the adiabatic potential H, and their explicit form can be found in appendix 3.

Because of the translational symmetry parallel to the layers we may write $\delta \boldsymbol{P}$ as

$$\delta \boldsymbol{P}(x, t) = \exp[\mathrm{i}(\boldsymbol{k}_{\parallel} \cdot \boldsymbol{x} - \omega t)]\boldsymbol{p}(x) \tag{4.10a}$$

and

$$\delta \boldsymbol{E}^{\mathrm{m}}(x, t) = -\nabla \varphi^{\mathrm{m}}(x, t) \qquad \text{with} \qquad \varphi^{\mathrm{m}}(x, t) = \varphi(x) \exp[\mathrm{i}(\boldsymbol{k}_{\parallel} \cdot \boldsymbol{x} - \omega t)] \tag{4.10b}$$

where $\boldsymbol{k}_{\parallel} = (0, k_y, k_z)$. Because of the Maxwell equation (4.7*a*) $\delta \boldsymbol{E}^{\mathrm{m}}$ could be expressed as the gradient of a scalar potential φ^{m} in (4.10*b*). Since the heterostructure is periodic in the x direction, $\boldsymbol{p}(x)$ and $\varphi(x)$ satisfy the Bloch condition

$$\boldsymbol{p}(x + D) = \exp(\mathrm{i}k_{\perp}D)\boldsymbol{p}(x) \qquad \text{and} \qquad \varphi(x + D) = \exp(\mathrm{i}k_{\perp}D)\varphi(x) \tag{4.11}$$

where $k_{\perp}$ is the Bloch wavenumber.

To conclude this section we want to discuss briefly two more points:

(i) We have used the quasi-static Maxwell equations to describe the long-range dipolar interaction. In principle, one would have to evaluate the depolarisation field $\delta \boldsymbol{E}^{\mathrm{m}}$ from the complete set of Maxwell equations. However, the use of the quasi-static equations—and hence the decoupling of the optical modes from photon dynamics—is justified, whenever the photon frequency $\omega_{\mathrm{ph}} = ck/n$ (with the index of refraction n) is large compared with the soft-mode frequency ω_0

$$\omega_0 \ll ck/n. \tag{4.12}$$

This approximation, of course, is not valid for $\boldsymbol{k} \to 0$ and this explains the seemingly unphysical result that the soft-mode frequencies have no unique limit for $\boldsymbol{k} \to 0$ (cf section 4.4).

(ii) Finally we turn to the influence of free carriers on the optical spectrum. The longitudinal optical (LO) modes give rise to the macroscopic electric field $\delta \boldsymbol{E}^{\mathrm{m}}$ and, as a result, their frequencies are higher than the frequencies of the transverse optical (TO) modes for $\boldsymbol{k} \to 0$. Free carriers in the ferroelectrics can screen this field, reducing the gap between the LO and TO modes [14]. In the following we assume that the multilayer constituents are pure insulators and neglect the influence of free carriers.

4.3. Propagation of transverse optical modes

First we want to study the spectrum of those solutions of equation (4.6) which are purely transverse, $\nabla \cdot \delta \boldsymbol{P} = 0$, and hence produce no macroscopic depolarisation field. If $\nabla \cdot \delta \boldsymbol{P} \neq 0$, the long-range dipolar interaction becomes important and its influence on the spectrum will be discussed in the next section. We also assume $\gamma = 0$, postponing the discussion of damping to section 5. For arbitrary direction of the in-plane wavevector $\boldsymbol{k}_\parallel$ equation (4.6) consists of four coupled equations for the three components of the polarisation $p_i(x), i = x, y, z$, and the potential $\varphi(x)$. In general, these modes are neither purely transverse nor purely longitudinal. In order to discuss the physics of the transverse modes, we put $\boldsymbol{k}_\parallel = (0, 0, 0)$ for simplicity. Then p_y and p_z are purely transverse and the equation for p_z reads

$$m\omega^2 p_z(x) = (1/\chi_\parallel^{\mathrm{ad},e_0} - \partial_x c_1 \partial_x) p_z(x) \tag{4.13}$$

while $p_y(x)$ obeys the same equation provided $\chi_\parallel^{\mathrm{ad},e_0}$ is replaced by $\chi_\perp^{\mathrm{ad},e_0}$.

Before solving this equation, we want to discuss the boundary conditions, which the polarisation has to obey at the interfaces. The GL coefficients as well as the spontaneous polarisation $P_0(x)$ entering into (4.13) are space-dependent quantities. If the GL coefficients and their derivatives are continuous functions, then $p_z(x)$ and its derivative are continuous throughout the whole sample and we do not have to face the question of boundary conditions. However, we approximate the GL coefficients by step functions as was explained in section 2. We now derive for this form of GL coefficients the boundary conditions that connect p_z and its derivative across the interfaces at $x = D_1/2|_+ \equiv D_1/2 + \Delta$ and $x = D_1/2|_- \equiv D_1/2 - \Delta$. Because of the inequality $\Delta/\xi_\alpha \ll 1$ (cf section 2) we may assume that p_z itself is continuous across the interfaces. The condition on $\partial_x p_z$ can be found by integrating (4.13) across the interface $\int_{D_1^{1/2}|_-}^{D_1^{1/2}|_+} \ldots \mathrm{d}x$

$$[-c_1 \partial_x p_z]_{D_1^{1/2}|_-}^{D_1^{1/2}|_+} \sim \mathrm{O}(p_z a \Delta). \tag{4.14a}$$

For small transition regions Δ of the GL parameters the right-hand side of (4.14*a*) may be neglected and one thus obtains the desired boundary conditions

$$[p_z]_{D_1^{1/2}|_-}^{D_1^{1/2}|_+} = 0 \qquad \text{and} \qquad [-c_1 \partial_x p_z]_{D_1^{1/2}|_-}^{D_1^{1/2}|_+} = 0. \tag{4.14b}$$

We note that the conditions (4.14*b*) also assure the continuity of the energy current density $j_{E,x}$,

$$j_{E,x} = (\mathrm{d}h/\mathrm{d}(\partial_x p_z)) \partial_t \delta p_z \tag{4.15}$$

across the interfaces. Herein the potential density h is defined through $H = \int h \, \mathrm{d}^3 x$.

Equation (4.13) is similar to—but not identical with—a Schrödinger equation for a particle with space-dependent mass. The temperature, which enters via the local susceptibility $\chi_\parallel^{\mathrm{ad},e_0}(T, x)$, appears as a parameter in the 'Hamiltonian'. Figure 5 shows the soft-mode spectrum resulting from equation (4.14) as a function of temperature and Bloch wavenumber $k_\perp$. The spectrum has gaps at wavenumbers $k_\perp = n\pi/D$, as is expected for a periodic structure. It is also clear that the eigenfrequencies change discontinuously at the transition temperature T_c, because the system undergoes a phase transition of first order. Further we note that the bands are flat for low energies and only the high energy levels show strong dispersion.

In order to understand the bandwidths we first indicate how the dispersion relation and its gaps are computed. Adopting the general treatment of [15] we determine even

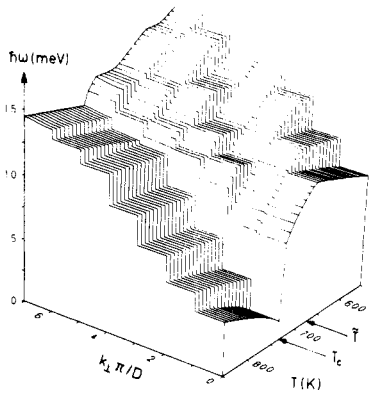

Figure 5. Soft-mode dispersion relation of the p_z component, equation (4.13), as a function of wavevector $\boldsymbol{k} = (k_\perp, 0, 0)$ and temperature. Parameters as in figure 2.

and odd one-cell solutions $g(\omega, x)$ and $u(\omega, x)$ of (4.13). In terms of these the dispersion relation follows from

$$\cos(k_\perp D) = 1 + 2u(\omega, D/2)\partial_x g(\omega, D/2)c_2/W \tag{4.16}$$

with the Wronskian $W = c_{1,1}g(\omega, 0)\partial_x u(\omega, 0)$.

Let us first consider the paraelectric temperature region $T > T_c$, where $P_0(x) = 0$. Then the potential term $1/\chi_\parallel^{\mathrm{ad},e_0}(x)$ has a step form and the solutions of (4.13) are elementary. Using the boundary conditions derived above one finds

$$g(\omega, x) = \begin{cases} \cos(p_1 x) - & \text{for } 0 \leqslant x \leqslant \dfrac{D_1}{2} \\ \cos\left(\dfrac{p_1 D_1}{2}\right)\cos\left[p_2\left(x - \dfrac{D_1}{2}\right)\right] & \\ -\dfrac{c_{1,1}p_1}{c_{1,2}p_2}\sin\left(\dfrac{p_1 D_1}{2}\right)\sin\left[p_2\left(x - \dfrac{D_1}{2}\right)\right] & \text{for } \dfrac{D_1}{2} \leqslant x \leqslant \dfrac{D}{2} \end{cases} \tag{4.17}$$

where

$$p_\alpha = \left(\frac{m_\alpha}{c_{1,\alpha}}(\omega^2 - \omega_{\mathrm{TO},\alpha}^2)\right)^{1/2} \qquad \alpha = 1, 2 \tag{4.18}$$

and the bulk soft-mode frequencies $\omega_{\mathrm{TO},\alpha}$ are defined by

$$\omega_{\mathrm{TO},\alpha} = (1/m_\alpha \chi_{\parallel,\alpha}^{\mathrm{ad},e_0})^{1/2}. \tag{4.19}$$

The odd solutions are found by replacing $\cos(p_1 x)$, $\cos(p_1 D/2)$ and $\sin(p_1 D_1/2)$ in (4.17) by $\sin(p_1 x)$, $\sin(p_1 D_1/2)$ and $-\cos(p_1 D_1/2)$, respectively. These expressions are also valid for purely imaginary p_α with a corresponding change of $\cos(p_\alpha x)$ into $\cosh(p_\alpha x)$, etc. The excitations can propagate in a particular layer α as long as $p_\alpha^2 > 0$. Otherwise they decay exponentially within the length $1/|p_\alpha|$ in this layer. Therefore, the form of the mode depends crucially on the signs of p_α^2, i.e. on the relation between the frequencies ω, $\omega_{\mathrm{TO},1}$ and $\omega_{\mathrm{TO},2}$. In figure 6 we have plotted the temperature dependence of the bulk frequencies $\omega_{\mathrm{TO},\alpha}(T)$. One sees that for the parameters chosen we have $\omega_{\mathrm{TO},2}(T) < \omega_{\mathrm{TO},1}(T)$ in the paraelectric temperature region $T > T_{c,2} \simeq T_c$. Therefore at temperatures $T > T_c$ and energies in the region $\omega_{\mathrm{TO},2} < \omega < \omega_{\mathrm{TO},1}$ the modes are localised in the layers 2 and decay exponentially into the layers 1. Consequently the bands are flat and their width depends on the overlap of the wavefunctions and behaves

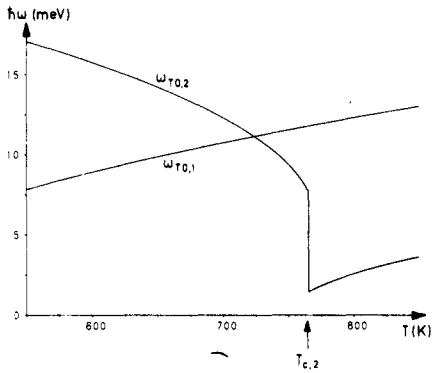

Figure 6. Temperature dependence of the bulk soft-mode frequencies $\omega_{TO,\alpha}(k=0)$, $\alpha=1,2$, equation (4.19).

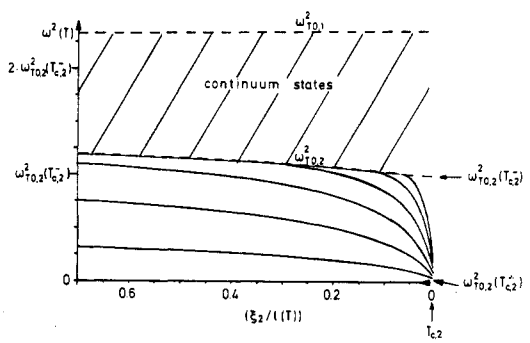

Figure 7. The six lowest eigenfrequencies (full curves) of the interface bound states of equation (4.13) for $k_\perp = k_\parallel = 0$ as a function of the scaled temperature within the temperature intervals $(T_{c,2} - 4.8\,\mathrm{K}) \leqslant T \leqslant T_{c,2}$. The broken curves represent the two bulk soft-mode frequencies. $D_1/\xi_1(T_{c,2}) = D_2/\xi_2(T_{c,2}) \to \infty$.

as $\exp(-|p_1|D_1)$ in this frequency region. Only for high frequencies $\omega > \omega_{TO,2}$ does the soft mode propagate through both layers giving rise to a finite bandwidth, as can be seen from figure 5.

Below the transition temperature T_c the polarisation profile $P_0(x)$ has a complex form and in general it is not possible to derive simple analytical expressions for the one-cell solutions g and u. Then the dispersion relation has to be calculated numerically. However, to get a qualitative understanding of the spectrum, let us approximate $P_0(x)$ by the step function

$$P_0(x) \simeq \sum_{n=-\infty}^{\infty} P_{b,2}\Theta[\tfrac{1}{2}D_2 - |x - (n+\tfrac{1}{2})D|] \tag{4.20}$$

which means that the polarisation assumes its bulk value $P_{b,2}$ in the layers 2 and vanishes in the layers 1. Then the functions g and u are given again by the expressions (4.16) and (4.17). As can be seen from figure 6, $\omega_{TO,1} < \omega_{TO,2}$ holds in the temperature region $T < 722\,\mathrm{K} < T_c$ for the chosen parameters. Therefore the modes at these temperatures, whose energies lie in the interval $\omega_{TO,1} < \omega < \omega_{TO,2}$, are confined to the layers 1. We see that, depending upon the temperature, the modes are confined either to the layers 1 or 2. Within the approximation (4.20) this change of mode type happens at the temperature $T = 722$ K. In section 5, we will show how this temperature dependence of the modes is reflected in the lineshape of the dynamic correlation function.

Actually the true polarisation profile (cf figure 3) gives rise to a space dependence of the 'potential energy' $1/\chi_\parallel^{ad,e_0}(x)$ in equation (4.13) that deviates from the simple step form at the interfaces. We now want to study how the inhomogeneity of the polarisation at the interfaces derived in section 3.3 influences the spectrum and the form of the modes. To this end the true polarisation profile has been inserted into (4.13), which has been solved numerically for the case of infinitely thick layers $D_1 = D_2 = \infty$, representing the special case of two adjacent semi-infinite materials 1 and 2, and for temperatures in the region $T_2 \ll T \leqslant T_c$. The lowest modes are shown in figure 7. There exist modes with

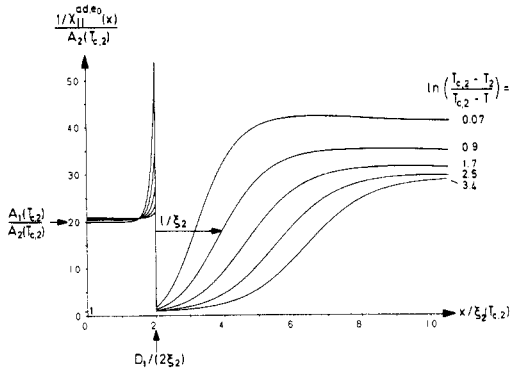

Figure 8. Potential energy $1/\chi_{\parallel}^{ad,e_0}(x)$ for several values of the temperature as indicated in the figure. Parameters as in figure 7.

frequencies $\omega < \min(\omega_{TO,1}, \omega_{TO,2})$ below the 'continuum'. To understand the nature of these modes, let us consider the potential term $1/\chi_{\parallel}^{ad,e_0}(x)$ in the 'Schrödinger equation' (4.13), which is plotted in figure 8 for several values of temperature. We see that there are potential wells within the layers 2 located at the interfaces. The modes with $\omega < \min(\omega_{TO,1}, \omega_{TO,2})$ can be understood as interface modes; i.e. bound states of these potential wells. Concerning the form of the potential wells, the following conclusions can be drawn from the analytical form of $P_0(x)$, as discussed in section 3:

(i) The width of the well is proportional to the length, l, equation (3.14*b*), and hence diverges logarithmically with $T_{c,2} - T$.

(ii) The bottom of the well is approximately given by $1/\chi_{\parallel}^{ad,e_0}(D_1/2|_+) \simeq A_2(T_{c,2})$.

(iii) The well is confined to the left at $x = D_1/2$ by a barrier of height

$$1/\chi_{\parallel}^{ad,e_0}(D_1/2|_-) \simeq 1/\chi_{\parallel,1}^{ad,e_0}(T = T_{c,2}) = A_1(T_{c,2})$$

and to the right at $x \sim D_1/2 + l$ by a barrier of height

$$1/\chi_{\parallel}^{ad,e_0}(D/2) \simeq 1/\chi_{\parallel,2}^{ad,e_0}(T = T_{c,2}).$$

In figure 7 we have plotted the lowest-lying eigenfrequencies ω_n, $n = 1, 2, \ldots$, of this potential instead of the temperature as a function of the temperature-dependent length $l(T)$. In the case of large well widths $l(T) \gg \xi_2$ the temperature dependence of the eigenvalues $\omega_n^2(T)$ can be understood in analogy with the energy levels of a square-well potential, for which one has

$$m_2[\omega_n^2(T) - \omega_0^2(T)] \sim c_{1,2}\left(\frac{n\pi}{l(T)}\right)^2 \sim 4A_2(T_{c,2})(n\pi)^2 \ln^{-2}\left(\frac{T_{c,2} - T_2}{T_{c,2} - T}\right). \tag{4.21}$$

It should be noted, however, that $l(T)$ always has a finite upper bound, given by its value at the transition temperature $l(T_c)$, equation (3.16). Consequently the limiting case $l(T) \gg \xi_2$ can only be realised for large layer thicknesses D_2, i.e. $\ln(D_2/\xi_2) \gg 1$. Of course the expression (4.21) is only valid for energies within the potential well, i.e. $\omega < \min(\omega_{TO,1}, \omega_{TO,2})$.

Concerning these interface modes we further note the following:

(i) The number N of bound states increases with decreasing temperature difference $T_c - T$, as follow directly from equations (4.21).

(ii) In the limit $D_\alpha \gg \xi_\alpha$ the frequencies of these interface modes are independent of the layer thicknesses D_α. Furthermore, they are twofold degenerate, because each unit cell contains *two* interfaces.

4.4. Influence of the dipolar interaction on the spectrum

In this section we study the influence of the long-range dipolar interaction on the phonon spectrum. Contact will also be made to previous theories [16–19], which take into account only the dipolar interaction and neglect the short-range elastic forces. We restrict ourselves to temperatures in the paraelectric phase $T > T_c$, and choose $\boldsymbol{k}_\parallel = (0, k_y, 0)$. From equation (4.6) we then deduce three coupled equations for the components p_x, p_y and φ, which read

$$m\omega^2 \begin{pmatrix} p_x(x) \\ p_y(x) \end{pmatrix} = \begin{pmatrix} \partial_x \\ \mathrm{i}k_\parallel \end{pmatrix} \varphi(x) + \begin{pmatrix} 1/\chi_\perp^{\mathrm{ad},e_0} + c_1 k_\parallel^2 - \partial_x(c_1 + c_2)\partial_x & \mathrm{i}k_\parallel \partial_x(-c_2 + c_3) \\ \mathrm{i}k_\parallel(-c_2 + c_3)\partial_x & 1/\chi_\perp^{\mathrm{ad},e_0} + (c_1 + c_2)k_\parallel^2 - \partial_x c_1 \partial_x \end{pmatrix} \times \begin{pmatrix} p_x(x) \\ p_y(x) \end{pmatrix} \tag{4.22a}$$

and

$$(\partial_x \varepsilon_\infty \partial_x - k_\parallel^2 \varepsilon_\infty)\varphi(x) = 4\pi[\partial_x p_x(x) + \mathrm{i}k_\parallel p_y(x)]. \tag{4.22b}$$

The solutions of (4.22) in general give rise to a macroscopic depolarisation field $\delta \boldsymbol{E}^{\mathrm{m}} = (-\partial_x, -\mathrm{i}k_\parallel, 0)\varphi$.

As in the preceding section we obtain from these equations effective boundary conditions for p_x, p_y, φ and their derivatives at the interfaces, which now read

$$[-(c_1 + c_2)\partial_x p_x + \mathrm{i}(c_3 - c_2)k_\parallel p_y]_{D_{1/2}}^{D_{1/2}}|_-^+ = 0 \tag{4.23a}$$

$$[-c_1 \partial_x p_y]_{D_{1/2}}^{D_{1/2}}|_-^+ = 0 \tag{4.23b}$$

$$[\varepsilon_\infty \partial_x \varphi + 4\pi \partial_x p_x]_{D_{1/2}}^{D_{1/2}}|_-^+ = 0 \qquad \text{and} \qquad [\varphi]_{D_{1/2}}^{D_{1/2}}|_-^+ = 0. \tag{4.23c}$$

Equation (4.23*c*) just expresses the continuity of the normal component of the displacement field $\delta \boldsymbol{D} = \varepsilon_\infty \delta \boldsymbol{E}^{\mathrm{m}} + 4\pi \delta \boldsymbol{P}$ and the continuity of the tangential component of $\delta \boldsymbol{E}^{\mathrm{m}}$.

The numerically calculated spectrum of equation (4.22) in the limit of very small wavenumbers $k_\perp D/\pi \ll 1$ and $k_\parallel D/\pi \ll 1$ is represented in figure 9 by the full curves. The parallel wavevector is fixed $k_\parallel = 0.01\pi/D$. From figure 9(*a*) the limits $k_\perp/k_\parallel \to 0$ and $k_\parallel/k_\perp \to 0$ can be read off from the branches to the left and to the right of $k_\parallel$. Modes the frequency of which are analytically in $\boldsymbol{k}$ are completely flat. We see that for some branches of the soft-mode frequencies the limiting value $\boldsymbol{k} \to 0$ is not unique but depends upon the propagation direction $\boldsymbol{k}/|\boldsymbol{k}|$, i.e. on the ratio between $k_\parallel$ and $k_\perp$. For smaller values of the stiffness constants c_i, this directional dependence in the limit $\boldsymbol{k} \to 0$ would be even more pronounced, as is demonstrated in figure 9(*b*), where the replacement $c_\alpha \to c_\alpha/10$ is made.

In order to understand this behaviour, let us consider the dipolar limit of the disordered phase, i.e. put $c_1(x) = c_2(x) = c_3(x) = 0$. Then equation (4.6) defines a frequency- and x-dependent dielectric tensor $\boldsymbol{\varepsilon}(x, \omega) = \varepsilon(x, \omega) \cdot \mathbf{1}$ and together with Maxwell's equation (4.7) one derives the relation

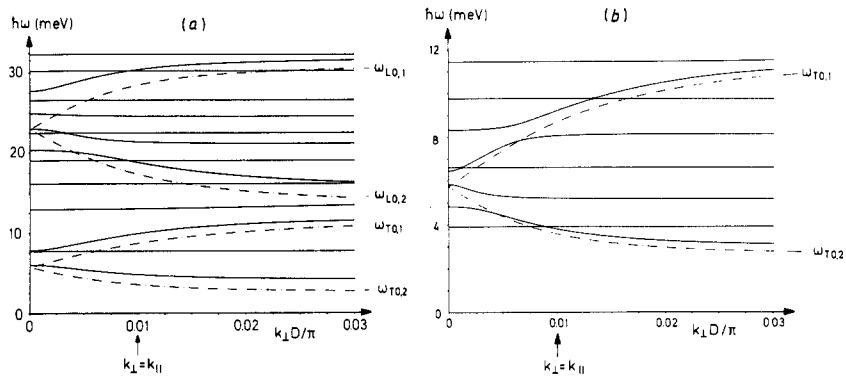

Figure 9. (*a*) Soft-mode frequencies as a function of $k_\perp D/\pi$ for $k_\parallel D/\pi = 0.01$ and $D_1 = D_2 = 20$ Å. The full curves are the solutions of equation (4.22); the chain curves are the solutions for the pure dipolar case. (*b*) Soft-mode frequencies as in (*a*) but with reduced stiffness coefficients $c_{1,\alpha} \to c_{1,\alpha}/10$ and $c_{2,\alpha} \to c_{2,\alpha}/10$.

$$[\partial_x \varepsilon(x, \omega)\partial_x - k_\parallel^2 \varepsilon(x, \omega)]\varphi(x) = 0 \tag{4.24}$$

for the electrostatic potential. Within each layer the dielectric function assumes the uniform values

$$\varepsilon_\alpha(\omega) = \varepsilon_{\infty,\alpha}\left(\frac{\omega^2 - \omega_{LO,\alpha}^2}{\omega^2 - \omega_{TO,\alpha}^2}\right) \qquad \alpha = 1, 2. \tag{4.25}$$

Equation (4.24) describes long-wavelength phonons in any dielectric heterostructure, such as for example in the semiconducting GaAs/AlAs superlattices [16]. The solutions of (4.24) are known [16–19], e.g. one finds for the dispersion relation the implicit expression

$$\frac{\cos(k_\perp D) - \cosh(k_\parallel D_1)\cosh(k_\parallel D_2)}{\sinh(k_\parallel D_1)\sinh(k_\parallel D_2)} = \frac{1}{2}\left(\frac{\varepsilon_1(\omega)}{\varepsilon_2(\omega)} + \frac{\varepsilon_2(\omega)}{\varepsilon_1(\omega)}\right). \tag{4.26}$$

Equation (4.26) gives rise to four frequency branches, which are exhibited in figure 9 by the chain curves. The comparison of full and chain curves reveals that the directional dispersion of the phonon frequencies is a dipolar effect.

In the limit of thick layers, $k_\parallel D_\alpha \gg 1$, $\alpha = 1, 2$, the solutions of (4.24) take the form [17]

$$\varphi(x) = \exp(-k_\parallel|x - D_1/2|) + \exp(ik_\perp D)\exp(-k_\parallel|x + D_1/2|) \qquad \text{for } |x| \leqslant D/2. \tag{4.27}$$

These are the so-called Fuchs–Kliever interface modes [20]. It is notable that these Fuchs–Kliever modes result from the dipolar interaction, while the second type of interface modes, discussed in section 4.3, had its origin in the special form of the inhomogeneous polarisation in a system with a phase transition of first order.

To conclude the discussion of the phonon dynamics in the ferroelectric heterostructure, it is worth comparing it with the dipolar magnon dynamics in the ferromagnetic heterostructure [4]. The phonon problem may be mapped onto the magnon problem by substituting $\boldsymbol{P}_0 \to \boldsymbol{M}_0$, $\delta\boldsymbol{E}^m \to \delta\boldsymbol{H}^m$ and $\varepsilon \to \mu$, where μ is the Polder tensor. However, there are characteristic differences resulting from the different nature of the polarisation

and magnetisation vectors. The magnetisation $\boldsymbol{M}_0$ is an axial, the polarisation $\boldsymbol{P}_0$ a polar vector.

(i) As a result the phonon equation of motion (4.6) is invariant under the reflection σ_x because of $\sigma_x \boldsymbol{P}_0 = \boldsymbol{P}_0$. This is not true for the magnetic case, where $\sigma_x \boldsymbol{M}_0 = -\boldsymbol{M}_0$. Consequently, the electrostatic potential has definite parity for Bloch wavenumbers at the zone boundary $k_\perp = n\pi/D$ [15], while the magnetostatic potential is asymmetric and is localised around only one of the two interfaces in the unit cell.

(ii) The vectors $(\boldsymbol{P}_0, \boldsymbol{k}_\parallel)$ transform under time reversal T into $(\boldsymbol{P}_0, -\boldsymbol{k}_\parallel)$. Therefore the same electrostatic potential $\varphi(x)$ appears for $\boldsymbol{k}_\parallel$ as well as for $-\boldsymbol{k}_\parallel$. On the other hand, because of $T\boldsymbol{M}_0 = -\boldsymbol{M}_0$, this does not hold for a magnetic system. Here the form of the modes depends upon $\mathrm{sgn}(k_y)$. This different behaviour under time reversal is clearly seen in inelastic light scattering on semi-infinite media. While in a scattering experiment on a dielectric structure one sees the Stokes *and* anti-Stokes lines, one of these lines is forbidden in the magnetic system.

5. Dynamic correlation functions

In this section we evaluate the dynamic correlation function $C_{ij}(\boldsymbol{x}, \boldsymbol{x}, \omega)$

$$C_{ij}(\boldsymbol{x}, \boldsymbol{x}, \omega) = \langle \delta P_i(\boldsymbol{x}, \omega) \delta P_j(\boldsymbol{x}, -\omega) \rangle \tag{5.1}$$

where

$$\delta \boldsymbol{P}_i(\boldsymbol{x}, \omega) = \int \delta \boldsymbol{P}_i(\boldsymbol{x}, t) \exp(\mathrm{i}\omega t)\, \mathrm{d}t \tag{5.2}$$

which may be probed by inelastic light and neutron scattering experiments.

Owing to the translational invariance in the film planes the correlation function can be written in the form

$$C_{ij}(\boldsymbol{x}, \boldsymbol{x}, \omega) = \frac{1}{(2\pi)^4} \int C_{ij}(x, x', \boldsymbol{q}_\parallel, \omega) \exp[\mathrm{i}\boldsymbol{q}_\parallel \cdot (\boldsymbol{x}_\parallel - \boldsymbol{x}'_\parallel)]\, \mathrm{d}\boldsymbol{q}_\parallel \tag{5.3}$$

with $\boldsymbol{x} = (x, \boldsymbol{x}_\parallel)$ and $\boldsymbol{q} = (q, \boldsymbol{q}_\parallel)$. The classical fluctuation–dissipation theorem relates the correlation functions $C_{ij}(x, x', \boldsymbol{q}_\parallel, \omega)$ to the linear response functions $G_{ij}(x, x', \boldsymbol{q}_\parallel, \omega)$ through

$$C_{ij}(x, x', \boldsymbol{q}_\parallel, \omega) = \frac{k_\mathrm{B} T}{\mathrm{i}\omega} [G_{ij}(x, x', \boldsymbol{q}_\parallel, \omega) - G^*_{ji}(x', x, \boldsymbol{q}_\parallel, \omega)]. \tag{5.4}$$

The latter describes the response of the polarisation $\delta \boldsymbol{P}(x, \boldsymbol{q}_\parallel, \omega)$ to a weak external electric field $\delta \boldsymbol{E}_{\mathrm{ext}}(x, \boldsymbol{q}_\parallel, \omega)$

$$\langle \delta P_i(x, \boldsymbol{q}_\parallel, \omega) \rangle = \int G_{ij}(x, x', \boldsymbol{q}_\parallel, \omega) \delta E_{j,\mathrm{ext}}(x', \boldsymbol{q}_\parallel, \omega)\, \mathrm{d}x' \tag{5.5}$$

and can be calculated from the equation of motion (4.6).

For simplicity we will consider in the following only the case $\boldsymbol{q}_\parallel = 0$ and will omit the argument $\boldsymbol{q}_\parallel$ in the ensuing expressions. Then the system (4.6) is invariant under the reflection $R = \sigma_y$ and the rotation $R = C_{2x}$ so that the response matrix is diagonal, $G_{ij} =$

$\delta_{ij}G_{ii}$. Furthermore, from the symmetry of the equations of motion under time reversal [21] it follows that

$$G_{ij}(x, x', \omega) = G_{ji}(x, x', \omega). \tag{5.6}$$

With (5.6) we may rewrite the fluctuation–dissipation theorem (5.4) for the diagonal component in the form

$$C_{ii}(x, x', \omega) = \frac{2k_B T}{\omega} \mathcal{I}(G_{ii}(x, x', \omega)) \qquad i = x, y, z. \tag{5.7}$$

Let us consider the zz component of the response function. From (4.6) one deduces

$$[-m(\omega^2 + i\gamma\omega) + \hat{g}(x)]G_{zz}(x, x', \omega) = \delta(x - x') \tag{5.8a}$$

with the linear operator

$$\hat{g}(x) = 1/\chi_{\parallel}^{\mathrm{ad},e_0} - \partial_x c_1 \partial_x. \tag{5.8b}$$

The solution of (5.8a) is well known [22] and may be expressed by the eigenfunctions $p_n(x, k_\perp, \omega)$ and eigenvalues $\varepsilon_n(k_\perp, \omega)$ of the eigenvalue problem

$$[-m\varepsilon_n^2(k_\perp, \omega) - im\gamma\omega + \hat{g}(x)]p_n(x, k_\perp, \omega) = 0. \tag{5.9a}$$

Here the $p_n(x, k_\perp, \omega)$ satisfy the Bloch condition

$$p_n(x + D, k_\perp, \omega) = \exp(ik_\perp D)p_n(x, k_\perp, \omega). \tag{5.9b}$$

Then the response function may be written as

$$G_{zz}(x, x', \omega) = \lim_{L\to\infty} \sum_{n,k_\perp} \frac{p_n(x', -k_\perp, \omega)p_n(x, k_\perp, \omega)}{[\varepsilon_n^2(k_\perp, \omega) - \omega^2]\langle p_n | p_n\rangle} \tag{5.10}$$

where $k_\perp$ assumes the discrete values $k_\perp = 2\pi m/L$, $m \in \mathbf{Z}$, and the scalar product is defined as

$$\langle p_n | p_n\rangle = \frac{1}{L}\int_0^L m(x)p_n(x, -k_\perp, \omega)p_n(x, -k_\perp, \omega)\,\mathrm{d}x. \tag{5.11}$$

In scattering experiments one measures the Fourier transform of the correlation functions

$$C_{zz}(q_\perp, \omega) = \iint C_{zz}(x, x', \omega)\exp[-iq_\perp(x - x')]\,\mathrm{d}x\,\mathrm{d}x' \tag{5.12}$$

which we have evaluated numerically. Its energy and temperature dependence is represented in figure 10. Here we have approximated the space dependence of the damping constant by a step function

$$\gamma(x) = \sum_{n=-\infty}^{\infty} \sum_{\alpha=1,2} \gamma_\alpha \Theta\{\tfrac{1}{2}D_\alpha - |x - [n + \tfrac{1}{2}(\alpha - 1)]D|\}. \tag{5.13}$$

For the constants γ_α we have chosen the temperature-independent values

$$\frac{\gamma_1}{\sqrt{2}\,\omega_{\mathrm{TO,PbTiO_3}}(T_{c,2})} = 1 \qquad \text{and} \qquad \frac{\gamma_2}{\sqrt{2}\,\omega_{\mathrm{TO,PbTiO_3}}(T_{c,2})} = 0.1 \tag{5.14}$$

which accounts for the fact that the damping is stronger in $BaTiO_3$ than in $PbTiO_3$ [23]. In figure 10 the correlation function is plotted as a function of T and ω with values of T

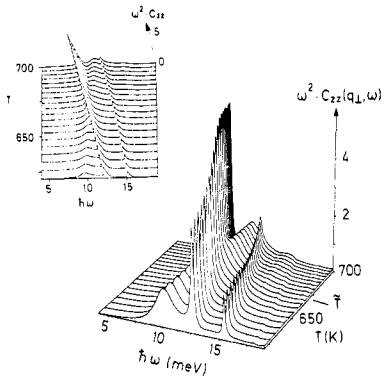

Figure 10. Correlation function $C_{zz}(q_\perp, \omega)$ (times ω^2) in arbitrary units as a function of ω and temperature. $q_\parallel = 0, q_\perp = \pi/(2D)$. The inset displays the same figure from above.

and ω within a certain interval. One clearly recognises in the peaks of the correlation function the band structure shown in figure 5, i.e. the peaks are situated at frequencies $\omega \simeq \varepsilon_n^0(k_\perp)$, where $\varepsilon_n^0(k_\perp)$ is the nth eigenvalue of equation (4.13), corresponding to a solution with Bloch wavenumber $k_\perp$. A prominent feature is that the linewidth of the lowest resonance at $\omega \simeq \varepsilon_1^0(k_\perp)$ is small for temperatures above $\tilde{T}$ and broad below, where $\tilde{T}$ is marked in figure 10. We want to show that this can be attributed to the temperature dependence of the shape of the modes, which was discussed in section 4.3. Let us for simplicity assume small damping constants $\gamma \ll \omega_{TO}$. For $\gamma = 0$ equation (5.9) reduces to equation (4.13). It has the solutions $p_n^0(x, k_\perp) = p_n^{0*}(x, -k_\perp)$ with the real eigenvalues $\varepsilon_n^0(k_\perp)$. For small γ, equation (5.9) may be solved perturbatively and one finds approximately

$$\varepsilon_n^2(k_\perp) = \varepsilon_n^0(k_\perp)[\varepsilon_n^0(k_\perp) - i\bar{\gamma}_n(k_\perp)] \tag{5.15a}$$

with the effective damping constant

$$\bar{\gamma}_n(k_\perp) = \int \gamma(x) m(x) |p_n^0(x, k_\perp)|^2 \, dx \Big/ \int m |p_n^0|^2 \, dx. \tag{5.15b}$$

Expanding $p_n^0(x, k_\perp)$ in the form

$$p_n^0(x, k_\perp) = \exp(ik_\perp x) \sum_{\nu = 0, \pm 1, \ldots} \rho_n(\nu, k_\perp) \exp(2\pi i x \nu / d) \tag{5.16}$$

we may rewrite the correlation function C_{zz}, equation (5.12), for frequencies ω close to ε_n^0 as

$$C_{zz}(q_\perp, \omega) \simeq k_B T \sum_n \frac{|\rho_n(\nu_0, k_\perp)|^2 \bar{\gamma}_n(k_\perp)}{\{[\varepsilon_n^0(k_\perp)^2 - \omega^2]^2 + [\bar{\gamma}_n(k_\perp)\varepsilon_n^0(k_\perp)]^2\}} \tag{5.17}$$

with $k_\perp = q_\perp \bmod(2\pi/D)$ and $\nu_0 = D(q_\perp - k_\perp)/2\pi$. The effective damping constant represents the halfwidth of the resonance at energy $\varepsilon_n^0(k_\perp)$. However, in section 4.3 it was shown that at high temperatures the low-energy modes p_n^0 are localised in the layers 2. Hence in this temperature region $\bar{\gamma}_n(k_\perp)$ is small for our choice of the parameter γ_2 (weak damping in $PbTiO_3$). At low temperatures the low-energy modes are localised within layers 1 and $\bar{\gamma}_n(k_\perp)$ becomes large due to the value of γ_1 (strong damping in $BaTiO_3$). The change of the type of the mode $p_1^0(x, k_\perp)$ occurs at the temperature $\tilde{T}$, marked in figure 10.

6. Summary

Sections 2 and 3 were devoted to the static properties of a ferroelectric heterostructure, undergoing a phase transition of first order. We explicitly took into account surface interactions and studied the influence of order-depressing surface parameters. From the general GL potential for polarisation and strain tensor we passed over to an effective potential for the polarisation, whose stationary states were determined. The GL equation was solved numerically. In the limit of large layer thicknesses, analytical results were presented for the following quantities:

(i) Polarisation profile. In the immediate vicinity below T_c unpolarised domains emerge from the weaker ferroelectric layers 1 into the stronger ferroelectric layers 2. The size of these domains increases logarithmically with the temperature difference $T_{c,2} - T$. This effect is due to the phase coexistence of the ordered ($P = P_{b,2}$) with the disordered ($P = 0$) phase in the bulk material 2 at its phase transition temperature $T = T_{c,2}$.

(ii) Transition temperatures. The phase transition temperature T_c of the heterostructure behaves for large thicknesses D_2 asymptotically as $T_{c,2} - T_c \sim D_2^{-1}$. The supercooling temperature T^{cool} follows a $T_2 - T^{cool} \sim D_2^{-2}$ law, where T_2 is the supercooling temperature of the bulk material 2. By looking at various limiting cases contact could be made with known results for films or semi-infinite media.

In section 4 we studied the dynamics of the soft mode, which is connected with the ferroelectric phase transition. First we evaluated the soft-mode dispersion in the absence of any long-range dipolar interaction. The lowest bands are almost dispersion-free and the corresponding modes are standing waves. These waves are localised in the layer constituents with the lower bulk soft-mode frequency. This mode confinement is also known for dielectric heterostructures [24]. A novelty, however, is the temperature dependence of the mode form and of the spectrum. Because the bulk soft-mode frequencies of the two layer constituents soften at different temperatures, the localisation of the modes in one or the other layer depends upon the temperature.

Furthermore, interface modes were found, which appear for temperatures close below T_c in sufficiently 'thick' layers $D_\alpha \gg \xi_\alpha$. They are a consequence of the special form of the inhomogeneous polarisation profile in a superlattice with a phase transition of first order. The number of these bound states increases with decreasing temperature difference $T_{c,2} - T$. These modes are twofold degenerate.

Finally we investigated the dispersion of the modes accompanied by a macroscopic electric field. Some of these modes show a directional dispersion for $\boldsymbol{k} \to 0$, i.e. the soft-mode frequency still depends on $\boldsymbol{k}/k$ in this limit. The comparison with the dipolar limit, where simple analytic expressions are known, reveals the dipolar origin of the directional dispersion. The differences between magnons in a ferromagnetic and phonons in the ferroelectric superlattice were discussed. These result from the fact that the magnetisation is represented by an axial and the polarisation by a polar vector.

In section 5 we studied the polarisation correlation function, which may be probed in light or neutron scattering experiments. The temperature dependence of the mode form can be seen in the lineshape, if the damping constants of the two layer constituents differ from each other, as is the case for $BaTiO_3$ and $PbTiO_3$. Then the linewidth of the correlation function depends upon in which sublattice the modes are localised and hence upon the temperature.

Acknowledgment

This work has been supported in part by the German Federal Minister for Research and Technology (BMFT) under Contract No 03-SC1TUM-0.

Appendix 1. Parameters

In the numerical calculations we used the following set of parameters, representing approximately bulk $BaTiO_3$ (subscript 1) and $PbTiO_3$ (subscript 2) [25–28]:

$A_1' = 0.028/T_1$, $A_2' = 0.064/T_2$, $T_1 = 381\,\mathrm{K}$, $T_2 = 749\,\mathrm{K}$, $C_{1,1} = 0.32\,\text{Å}^2$, $C_{1,2} = 0.89\,\text{Å}^2$, $C_{2,1} = 1.85\,\text{Å}^2$, $C_{2,2} = 5.12\,\text{Å}^2$, $C_{3,1} = 3.26\,\text{Å}^2$, $C_{3,2} = 9.02\,\text{Å}^2$, $B_{11,1} = 2.32 \times 10^{-14}[T(\mathrm{K}) - 436]\,\mathrm{cm^3\,erg^{-1}}$, $B_{11,2} = -4.56 \times 10^{-13}\,\mathrm{cm^3\,erg^{-1}}$, $B_{12,1} = 7.96 \times 10^{-13}\,\mathrm{cm^3\,erg^{-1}}$, $B_{12,2} = 2.70 \times 10^{-12}\,\mathrm{cm^3\,erg^{-1}}$, $B_{111,1} = 9 \times 10^{-23}\,\mathrm{cm^6\,erg^{-2}}$, $B_{111,2} = 2.85 \times 10^{-23}\,\mathrm{cm^6\,erg^{-2}}$, $B_{112,1} = 1.23 \times 10^{-22}\,\mathrm{cm^6\,erg^{-2}}$, $B_{112,2} = 1.65 \times 10^{-22}\,\mathrm{cm^6\,erg^{-2}}$, $c_{11,1} = 1.9 \times 10^{12}\,\mathrm{erg\,cm^{-3}}$, $c_{11,2} = 1.8 \times 10^{12}\,\mathrm{erg\,cm^{-3}}$, $c_{12,1} = 9.7 \times 10^{11}\,\mathrm{erg\,cm^{-3}}$, $c_{12,2} = 7.5 \times 10^{11}\,\mathrm{erg\,cm^{-3}}$, $q_{11,1} = 1.3$, $q_{11,2} = 0.7$, $q_{12,1} = -0.4$, $q_{12,2} = -0.3$, $c_{V,0,1}(T_{c,1}^+) = 24 \times 10^6\,\mathrm{erg\,cm^{-3}\,K^{-1}}$, $c_{V,0,2}(T_{c,2}^+) = 6 \times 10^7\,\mathrm{erg\,cm^{-3}\,K^{-1}}$, $\varepsilon_{\infty,1} = 76$, $\varepsilon_{\infty,2} = 123$, $m_1 = 0.9 \times 10^{-28}\,\mathrm{s^2}$ and $m_2 = 2.9 \times 10^{-28}\,\mathrm{s^2}$.

Furthermore the flexoelectric coefficients as well as the surface coefficients were assumed to vanish, i.e. $F_{ij,\alpha} = I = J = 0$.

Appendix 2. Ginzburg–Landau coefficients of the effective potential

The GL coefficients A, B_{ij}, s_{ij} and Q_{ij} of the effective potential G^X, equation (3.2), are connected with the original coefficients a, b_{ij}, c_{ij} and q_{ij} of the potential G, equation (2.1), by well known relations [6]:

$$A = a \qquad A' = a' \tag{A2.1a}$$

$$B_{111} = b_{111} \qquad B_{112} = b_{112} \qquad B_{123} = b_{123} \tag{A2.1b}$$

$$B_{11} = b_{11} + 2[-q_{11}^2(c_{11} + c_{12}) + 4q_{11}q_{12}c_{12} - 2q_{12}^2c_{11}]/\det \tag{A2.1c}$$

$$B_{12} = b_{12} + 2[q_{11}^2c_{12} - 2q_{11}q_{12}c_{11} + q_{12}^2(2c_{12} - c_{11})]/\det - q_{44}^2/c_{44} \tag{A2.1d}$$

$$s_{11} = (c_{11} + c_{12})/\det \qquad s_{12} = -c_{12}/\det \qquad s_{44} = 1/c_{44} \tag{A2.1e}$$

$$Q_{11} = [q_{11}(c_{11} + c_{12}) - 2q_{12}c_{12}]/\det \tag{A2.1f}$$

$$Q_{12} = (-q_{11}c_{12} + q_{12}c_{11})/\det \qquad Q_{44} = q_{44}/c_{44} \tag{A2.1g}$$

with

$$\det = (c_{11} - c_{12})(c_{11} + 2c_{12}). \tag{A2.2}$$

Owing to the flexoelectric coefficients we get further that

$$C_1 = c_1 - f_{44}^2/c_{44} \tag{A2.3a}$$

$$C_2 = c_2 - [f_{11}^2(c_{11} + c_{12}) + 2f_{12}^2c_{11} - 4f_{11}f_{12}c_{12}]/\det + f_{44}^2/c_{44} \tag{A2.3b}$$

$$C_3 = c_3 - (f_{11} - f_{12})^2/(c_{11} - c_{12}) \tag{A2.3c}$$

$$F_{11} = [f_{11}(c_{11} + c_{12}) - 2f_{12}c_{12}]/\det \tag{A2.3d}$$

$$F_{12} = (f_{12}c_{11} - f_{11}c_{12})/\det \qquad F_{44} = f_{44}/c_{44}. \tag{A2.3e}$$

Appendix 3. Adiabatic Ginzburg–Landau coefficients

The transition from the isothermal potential G to the adiabatic potential H, equation (4.3), leads to a transformation of the GL coefficients $b_{ij} \rightarrow b_{ij}^{ad}, \ldots$. Assuming a linear temperature dependence of the coefficients a and b_{11} we get [29]

$$b_{11}^{ad} - b_{11} = T(da/dT)^2/(3c_{V,0}) \tag{A3.1a}$$

$$b_{111}^{ad} - b_{111} = 2T(da/dT)(db_{11}/dT)/(5c_{V,0}). \tag{A3.1b}$$

Here $c_{V,0}$ is the specific heat in the unpolarised phase. All other GL coefficients remain unchanged.

Note that we have omitted the thermal expansion term $\sim -\alpha(T - T_0)(e_1 + e_2 + e_3)$ in the expression for the elastic energy G_2, equation (2.3*b*). The expansion coefficient α also gives rise to corrections in the adiabatic coefficients. These corrections are small, however, and may be neglected.

References

[1] Bauer G, Pascher H and Kriechbaum M 1987 *Phys. Scr.* T **19** 147
[2] Kriechbaum M, Ambrosch K E, Fantner E J, Clemens H and Bauer G 1984 *Phys. Rev.* B **30** 3394
[3] Murase K, Shimomura S, Takaoka S, Ishida A and Fujiyama H 1985 *Superlatt. Microstruct.* **1** 97
[4] Schwenk D, Fishman F and Schwabl F 1988 *Phys. Rev.* B **38** 11618
[5] Ginzburg V L 1960 *Fiz. Tverd. Tela* **2** 2031
[6] Mitsui T *et al* 1976 *An Introduction to the Physics of Ferroelectrics* (New York: Gordon and Breach) p 22
[7] Levanyuk A P and Minyukov S A 1981 *Ferroelectrics* **35** 227
[8] Ashcroft N W and Mermin N D 1976 *Solid State Physics* (New York: Holt, Rinehart and Winston) p 300
[9] Jona F and Shirane G 1962 *Ferroelectric Crystals* (Oxford: Pergamon) p 108
[10] Slonczewski J C and Thomas H 1970 *Phys. Rev.* B **1** 3599
[11] Falk F 1983 *Z. Phys.* B **51** 177
[12] Lipowsky R and Speth W 1983 *Phys. Rev.* B **28** 3983
[13] Tamura S and Wolfe J P 1987 *Phys. Rev.* B **35** 2528
[14] Cowley R A and Dolling G 1965 *Phys. Rev. Lett.* **14** 549
[15] Jones H 1975 *The Theory of Brillouin Zones and Electronic States in Crystals* (Amsterdam: North-Holland) p 25
[16] Sood A K, Menedez J, Cardona M and Ploog K 1985 *Phys. Rev. Lett.* **54** 2115
[17] Camley R E and Mills D L 1984 *Phys. Rev.* B **29** 1695
[18] Agranovich V M and Kravtsov V E 1985 *Solid State Commun.* **55** 85
[19] Pokatilov E P and Beril S I 1983 *Phys. Status Solidi* B **118** 567
[20] Fuchs R and Kliever K L 1965 *Phys. Rev.* A **140** 2076
[21] Landau L D and Lifschitz E M 1959 *Course of Theoretical Physics* vol 5 *Statistical Physics* (London: Pergamon) p 389
[22] Kamke E 1956 *Differentialgleichungen, Lösungsmethoden und Lösungen I* (Leipzig: Geest and Portig) p 246
[23] Burns G and Scott B A 1973 *Phys. Rev.* B **7** 3088
[24] Olego D J, Shahzad K, Cammack P A and Cornelissen H 1988 *Phys. Rev.* B **38** 5554
[25] Landolt-Börnstein 1981 *Ferroelectrics and Related Substances* vol 16a (Berlin: Springer) p 328
[26] Shirane G, Axe J D and Harada J 1970 *Phys. Rev.* B **2** 155
[27] Harada J, Axe J D and Shirane G 1971 *Phys. Rev.* B **4** 155
[28] Amin A, Haun M J, Badger B, McKinstry H and Cross L E 1985 *Ferroelectrics* **65** 107
[29] Grindlay J 1970 *An Introduction to the Phenomenological Theory of Ferroelectricity* (Oxford: Pergamon) p 171